

# Saccharide-Linked Ethynylpyridine Oligomers: Primary Structures Encode Chiral Helices

Hajime Abe,<sup>\*,†,‡</sup> Daisuke Murayama,<sup>†</sup> Fumihiko Kayamori,<sup>†</sup> and Masahiko Inouye<sup>\*,†</sup>

Graduate School of Pharmaceutical Sciences, University of Toyama, Toyama 930-0194, Japan, and PRESTO, JST, Tokyo 102-0075, Japan

Received July 1, 2008; Revised Manuscript Received July 10, 2008

**ABSTRACT:** A series of glycoside-linked oligomeric 2,6-pyridylene–ethynylene (*m*-ethynylpyridine) compounds were prepared and studied for their intramolecular chiral induction. The primary structure of the oligomers, such as the lengths of ethynylpyridine moieties and linkers and the types of terminal groups and linked glycosides, was varied. From circular dichroism (CD) and <sup>1</sup>H NMR analyses, it was found that the intramolecular hydrogen bonds between the glycoside and ethynylpyridine moieties induced the formation of higher-order, chiral helices of the oligomers. The sign and strength of CD signals for the helices were found to depend strongly on the length of ethynylpyridines and the types of terminal groups and glycosides. These results showed that the oligomers encode their higher-order structures in their primary structures.

## Introduction

In organisms, homeostasis is maintained by the contribution of various biopolymers such as proteins, nucleic acids, and polysaccharides. Various functions of the biopolymers are due to their chiral higher-order structures originated from their primary structures.<sup>1</sup> Sophisticated designs for primary structures of synthetic polymers have successfully constructed nature-mimetic and artificial higher-order structures such as helices, some of which are chiral.<sup>2</sup> Recently, several examples of chiral helical foldamers have been reported,<sup>2,3</sup> using strategies such as (1) introducing chiral centers on each repeating unit of the foldamer,<sup>4</sup> (2) connecting one chiral center at the end or middle of the foldamer with amplification of the chirality (sergeant–soldier effect),<sup>5,6</sup> and (3) offering a chiral template which associate with the foldamer intermolecularly.<sup>3g,6b,d,7–9</sup> The last strategy is based on host–guest chemistry between host foldamers and guest chiral templates, and the choice of the guest can tune the fine structure of the helix. However, unless the host–guest association is sufficiently strong, a large excess of the guest template must be added or the chirality of the host foldamer is lost. This situation could affect quantitative investigation of the structure of chiral helices. One solution for this problem is to bind chiral templates into host polymers at a suitable position through a covalent-bonding linker. Compared to intermolecular association, intramolecular bonds will reduce the entropic loss and reinforce the association. Recently, we have investigated 2,6-pyridylene–ethynylene (*m*-ethynylpyridine) polymers and oligomers as host molecules, which recognize saccharides<sup>10</sup> to form helical complexes (Figure 1A).<sup>9</sup> We decided to employ this chemistry for synthesizing *m*-ethynylpyridine oligomers that link covalently with saccharide templates to spontaneously produce stable helices. The sense, pitch, and size of the resulting helical structures varied according to the primary structure units of the oligomers. In other words, the primary structures of the oligomers encode their higher-order structures, just as the peptides do (Figure 1B).

## Results and Discussion

**Molecular Design of Oligomers.** Our design for the primary structure of saccharide-linked *m*-ethynylpyridine oligomers is

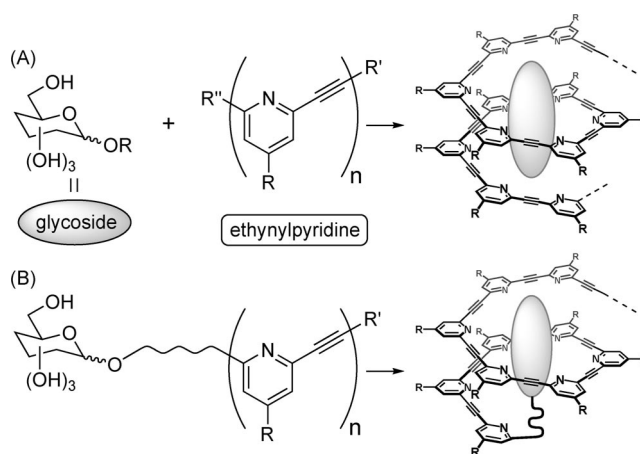


**Figure 1.** Helix formation of *m*-ethynylpyridine polymers and oligomers (A) with external glycosides by intermolecular association and (B) with covalently linked glycosides by intramolecular association.

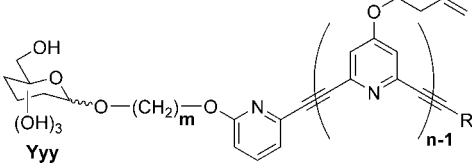
depicted in Table 1. The oligomers are composed of a saccharide template, an alkylene linker, an oligo(*m*-ethynylpyridine), and a terminal group. These components are organized by their lengths and types, and each assembly of the components is labeled **Yyy-*m*-*n*-R'** (Yyy: the type of saccharide templates; *m*: the length of methylene linkers; *n*: the number of pyridine rings, R': the type of terminal group). These saccharide-linked oligomers were synthesized to study the relationship between their primary and higher-order helical structures. The 3-butenyl groups at the 4-position of the pyridine rings were introduced for future chemical modifications. A control decamer lacking glycosides (**HO-3-10-TBS**) was also prepared.

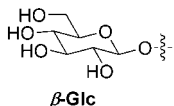
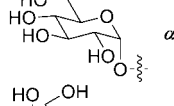
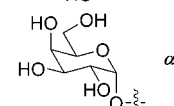
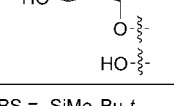
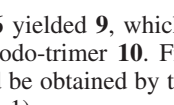
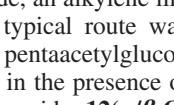
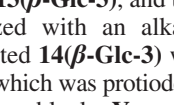
**Synthesis of the Oligomers.** The components described above were assembled into oligomers by the Sonogashira reaction, Fischer glycosidation, and Williamson synthesis. One crucial building block for synthesizing the oligomers is the ethynylpyridine tetramer **11**. Condensation of 2,6-dibromopyridin-4-ol (**1**) with 4-bromo-1-butene yielded **2**, and it was converted to diiodide **3** by halogen exchange.<sup>11</sup> Sonogashira coupling of the dibromide **2** with 3-methyl-1-buten-3-ol yielded mono- and disubstituted products **5** and **6** selectively, based on the choice of reaction conditions. Coupling of **5** with *tert*-butyldimethylsilylacetylene (TBSA) followed by detachment of acetone yielded monoprotected diethynylpyridine **8**. Deprotec-

\* Corresponding author: e-mail abeh@pha.u-toyama.ac.jp, Tel +81-76-434-7527, Fax +81-76-434-5049.

<sup>†</sup> University of Toyama.

<sup>‡</sup> PRESTO, JST.

**Table 1. Primary Structures and Abbreviations of Saccharide-Linked *m*-Ethynylpyridine Oligomers and a Control**


Yyy	oligomer Yyy- <i>m</i> - <i>n</i> -R'
 β-Glc	β-Glc-3-3-TBS
	β-Glc-3-6-TBS
	β-Glc-3-10-TBS
	β-Glc-3-10-H
	β-Glc-6-10-TBS
 α-Glc	β-Glc-3-14-TBS
	α-Glc-3-6-TBS
	α-Glc-3-10-TBS
 β-Gal	α-Glc-3-10-H
	α-Glc-3-14-TBS
	β-Gal-3-6-TBS
 α-Gal	β-Gal-3-10-TBS
	β-Gal-3-10-H
	β-Gal-3-14-TBS
 α-Man	α-Gal-3-6-TBS
	α-Gal-3-10-TBS
	α-Gal-3-10-H
 α-Man	α-Gal-3-14-TBS
	α-Man-3-6-TBS
	α-Man-3-10-TBS
 HO-3-10-TBS	α-Man-3-10-H
	α-Man-3-14-TBS
	HO-3-10-TBS

TBS = -SiMe<sub>2</sub>Bu-*t*

tion of **6** yielded **9**, which was treated with an excess of **3** to form diiodo-trimer **10**. Finally, the tetrameric building block **11** could be obtained by the reaction of **8** with an excess of **10** (Scheme 1).

The other key building block is **Yyy-*m*-2-H** consisting of a saccharide, an alkylene linker, and two pyridine rings (Scheme 2). The typical route was exemplified with **β-Glc-3-2-H** as follows: pentaacetylglucose was condensed with 3-bromopropan-1-ol in the presence of BF<sub>3</sub>·OEt<sub>2</sub> to yield a mixture of α- and β-glucosides **12(α/β-Glc-3)** (α/β ≈ 1:3). Then, the separated β-anomer **12(β-Glc-3)** was condensed with 6-iodo-2-pyridone<sup>12</sup> to yield **13(β-Glc-3)**, and the acetyl groups of **13(β-Glc-3)** were hydrolyzed with an alkaline solution to **14(β-Glc-3)**. The deprotected **14(β-Glc-3)** was coupled with **8** to yield **β-Glc-3-2-TBS**, which was protidesilylated to **β-Glc-3-2-H**. Other kinds of building blocks **Yyy-*m*-2-H** were also prepared by similar procedures using the corresponding starting glycosides.

Then, a series of oligomers listed in Table 1 were prepared from the building blocks by repeating Sonogashira coupling and protidesilylation in appropriate ways as shown in Scheme 3. The building block **Yyy-*m*-2-H** was coupled with **11** to yield hexamers **Yyy-*m*-6-TBS**. After protidesilylation, **Yyy-*m*-6-H** was coupled again with **11** to decamers **Yyy-*m*-10-TBS**, and one more expansion cycle yielded **Yyy-*m*-14-TBS**. Furthermore, **α-Man-3-10-TBS** was resolved into saccharide-free **HO-3-10-TBS** and used as a control.

**Comparison of Intramolecular (β-Glc-3-10-TBS) and Intermolecular (HO-3-10-TBS/β-Glc) Chiral Inductions.** Circular dichroism (CD) measurements were conducted to study higher-order structures of the oligomers. The red solid line in

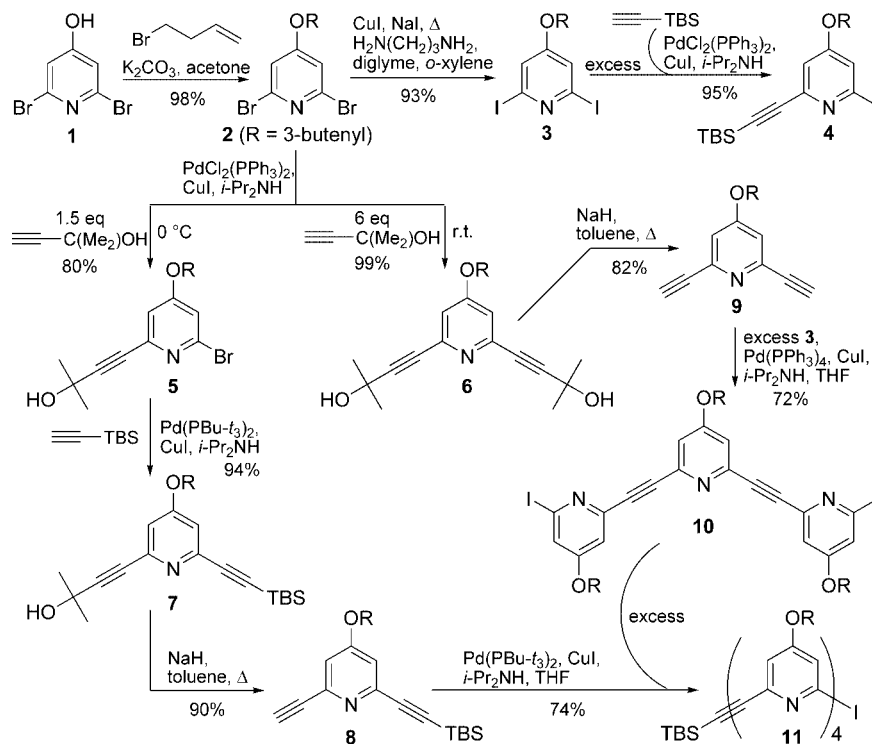
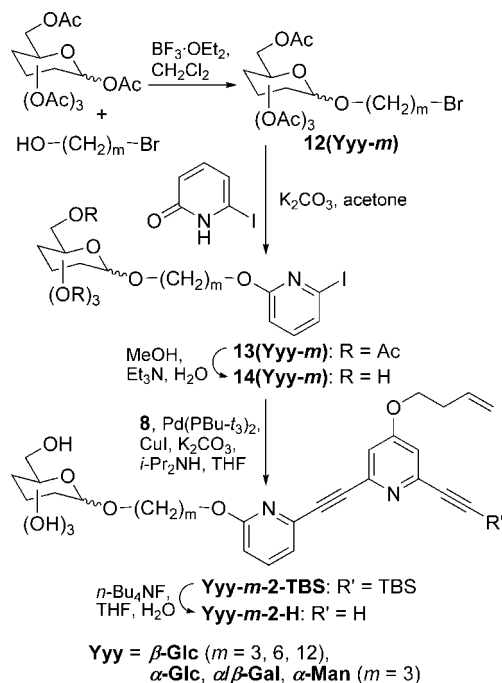
Figure 2 is the CD spectrum for a CH<sub>2</sub>Cl<sub>2</sub> solution of **β-Glc-3-10-TBS**, which shows a remarkably strong CD band around 340 nm. The oligomer **β-Glc-3-10-TBS** has a chiral center only in the glucoside template in its primary structure, and that template has no absorbance at ≥250 nm. On the other hand, the ethynylpyridine moiety is achiral by itself and has absorbance around 340 nm. Thus, the observed CD band should be due to chiral induction from the glucoside template to the ethynylpyridine moiety through hydrogen-bonding association. The shape of the CD spectrum of **β-Glc-3-10-TBS** closely resembles that of the induced CD spectrum for simple ethynylpyridine polymers treated with an excess of octyl β-D-glucopyranoside.<sup>9a,b</sup> Therefore, the higher-order structure of **β-Glc-3-10-TBS** proved to be similar to that resulting from the corresponding intermolecular combination. The addition of MeOH to a CH<sub>2</sub>Cl<sub>2</sub> solution of **β-Glc-3-10-TBS** suppressed the CD band because MeOH disturbs the hydrogen bonding between the glucoside and ethynylpyridine moieties (Figure 2, blue solid line).<sup>9a</sup>

In the above-mentioned molecular design, we expected the glycoside-linked oligomers to form intramolecular complexes as shown in Figure 1B. Therefore, we studied the effect of concentration on the UV-vis and CD spectra for **β-Glc-3-10-TBS** to determine whether the helix induction occurs via an intra- or intermolecular route. If the helix induction is due to an intermolecular association to some extent, the molar extinction coefficient and molar ellipticity will be dependent on the substrate concentration. The observed linearities for the absorbance and CD intensity of **β-Glc-3-10-TBS** against its concentration suggest that the oligomer exists predominantly as only one kind of CD-active species at concentration ≤2.0 × 10<sup>-4</sup> M (Figure 3). Thus, the oligomer was found to form an intramolecular hydrogen-bonding complex at that concentration. Three other types of oligomers **α-Man-3-6-TBS**, **α-Man-3-10-TBS**, and **α-Man-3-14-TBS** also showed similar linearities in UV-vis spectra (Figure S1 in Supporting Information). Therefore, the CD and UV-vis observation for a series of the oligomers described below should be attributed to intramolecular helix induction.

The advantage of covalent linking between the glucoside template and ethynylpyridine moieties was demonstrated by comparing CD spectra of **β-Glc-3-10-TBS** and the mixture of saccharide-free **HO-3-10-TBS** and octyl β-D-glucopyranoside (**β-Glc**). As shown by the broken lines in Figure 2, the equimolar mixture of **HO-3-10-TBS** and **β-Glc** showed no meaningful induced CD (black broken line), and even the use of a large excess of **β-Glc** caused only weak induced CDs (green broken line). The intermolecular association of **HO-3-10-TBS** with **β-Glc** would cause a serious entropic loss, and such loss does not exist in the case of **β-Glc-3-10-TBS**, the covalently linked oligomer.

#### Effects of Primary Structure of the Oligomers on CD.

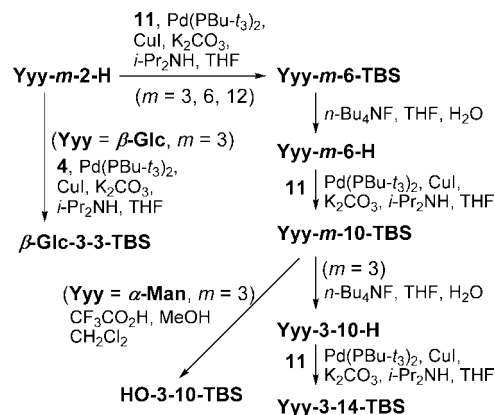
Next, we studied the effect of the primary structure of the oligomers on their higher-order structures in detail. For an easy comparison of the spectroscopic data, the concentration of each oligomer solution was normalized against the pyridine unit concentration. Parts A and B of Figure 4 display the CD spectra of a series of the β-glucoside oligomers **β-Glc-*m*-*n*-TBS** and desilylated **β-Glc-3-10-H** at a pyridine unit concentration of 1.5 × 10<sup>-3</sup> M. Table 2 summarizes molar ellipticities for the β-glucosides as well as other saccharide-linked oligomers. In experiments conducted to determine the effect of the linker length, the propylene-linked **β-Glc-3-10-TBS**, hexylene-linked **β-Glc-6-10-TBS**, and dodecylene-linked **β-Glc-12-10-TBS** showed similar CD spectra (Figure 4A). As we observed that the linker length do not play an important role in helix formation, only the oligomers possessing a propylene linker were used in

Scheme 1. Preparation of Tetrameric Building Block 11 (TBS = *tert*-Butyldimethylsilyl)Scheme 2. Preparation of a Saccharide-Linker Block Yyy-*m*-2-*H*<sup>a</sup>

<sup>a</sup> "Yyy" represents the kind of glycoside (see Figure 1).

the following experiments. In experiments conducted to determine the effect of the length of the ethynylpyridine moiety, the trimer **β-Glc-3-3-TBS** showed a very weak CD signal because it is too short to form a helical structure. Although the hexamer **β-Glc-3-6-TBS** is still short and shows a weak CD signal, the two longer oligomers **β-Glc-3-10-TBS** and **β-Glc-3-14-TBS** exhibited strong CD signals by forming chiral helical structures (Figure 4B). Thus, the variation in the lengths of the ethynylpyridine moiety strongly influenced the intensity of CD signals

Scheme 3. Preparation of Targeted Saccharide-Linked Oligomers



with the same sign. Furthermore, removal of the terminal TBS group was found to drastically weaken the CD intensity, as shown by the comparison between the CD intensities of **β-Glc-3-10-H** and **β-Glc-3-10-TBS**. This tendency was also seen in other saccharide-linked oligomers (Table 2).

The type of glycoside template was responsible for the sign of CD signals of the oligomers. Decamers linked with  $\alpha$ - and  $\beta$ -glucosides exhibited negative CD signals around 335 nm, while other decameric glycosides,  $\alpha$ - and  $\beta$ -galactosides and  $\alpha$ -mannoside, showed positive CD signals (Figure 5). The shapes of the CD signals for these decamers resemble qualitatively one another except the sign. Thus, a small structural change of only one OH group resulted in the reversal of the sign of the CD signals, which is due to the inversion of the sense of the helicity of the oligomers.

**Relationship between the Magnitude of Ellipticity and Hypochromism of the Oligomers.** For foldamers containing aromatic rings, it has been reported that the stabilization of helical structure occasionally caused hypochromism in their UV-vis absorbance because of an enforced intramolecular

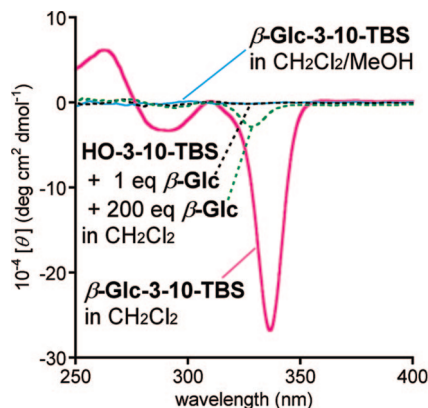


**Figure 2.** CD spectra of  $\beta$ -Glc-3-10-TBS and HO-3-10-TBS/ $\beta$ -Glc: (red solid)  $\beta$ -Glc-3-10-TBS ( $1.5 \times 10^{-4}$  M) in  $\text{CH}_2\text{Cl}_2$ ; (blue solid)  $\beta$ -Glc-3-10-TBS ( $1.5 \times 10^{-4}$  M) in  $\text{CH}_2\text{Cl}_2/\text{MeOH}$  (3:1); (black broken) HO-3-10-TBS ( $1.5 \times 10^{-4}$  M) +  $\beta$ -Glc ( $1.5 \times 10^{-4}$  M) in  $\text{CH}_2\text{Cl}_2$ ; and (green broken) HO-3-10-TBS ( $1.5 \times 10^{-4}$  M) +  $\beta$ -Glc ( $3.0 \times 10^{-2}$  M) in  $\text{CH}_2\text{Cl}_2$ . 25 °C, path length = 1 mm.

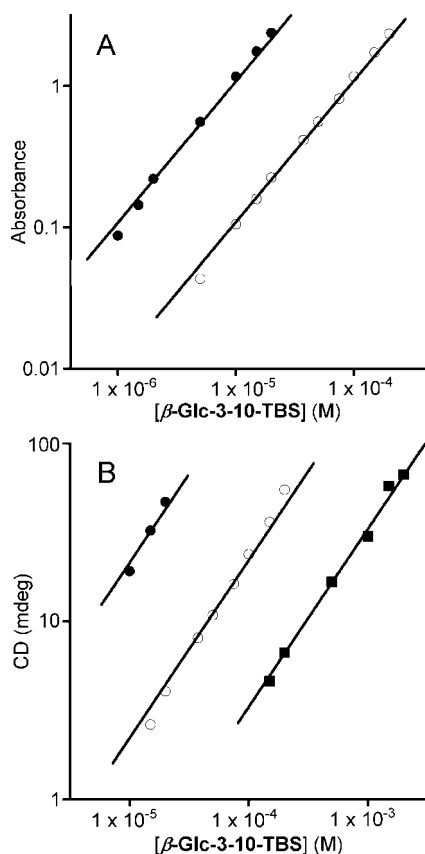


**Figure 3.** Relationship of concentration of  $\beta$ -Glc-3-10-TBS with (A) absorbance at 317 nm ( $1.0 \times 10^{-6}$ – $2.0 \times 10^{-4}$  M) and (B) CD at 340 nm ( $1.0 \times 10^{-5}$ – $2.0 \times 10^{-3}$  M) in  $\text{CH}_2\text{Cl}_2$  at 25 °C. Path length = 0.1 (filled square), 1 (open circle), or 10 mm (filled circle). Lines show proportional functions fit to the data.

$\pi$ -stacking interaction.<sup>4f,13</sup> The CD spectrum of the  $\alpha$ -mannoside-linked short hexamer  $\alpha$ -Man-3-6-TBS showed a noticeable shape, whereas other saccharide-linked hexamers showed only weak CD signals, similar to the above-mentioned  $\beta$ -Glc-3-6-TBS (Table 2). The  $\alpha$ -mannoside moiety was found to work well as a chiral template to form an intramolecular helical structure even in shorter oligomers. Therefore, we performed a systematic comparison of the intensities of CD and UV-vis spectra for various lengths of ethynylpyridine moiety using the data from a series of  $\alpha$ -Man-3-*n*-TBS at a pyridine unit

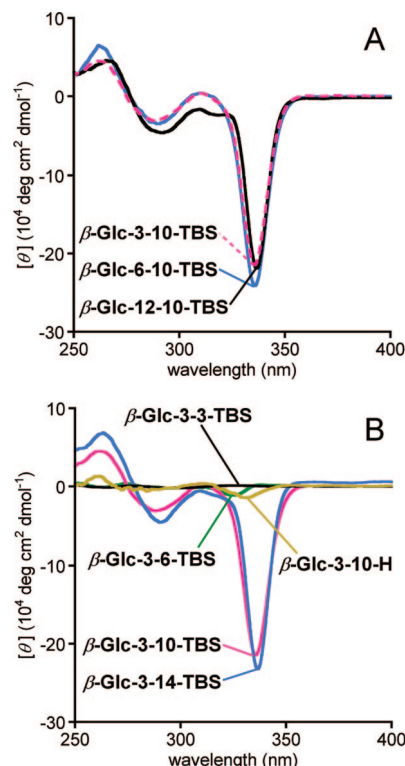


**Figure 4.** CD spectra of  $\beta$ -glucoside-linked oligomers. Pyridine unit concentration was set at  $1.5 \times 10^{-3}$  M in  $\text{CH}_2\text{Cl}_2$ , 25 °C, path length = 1 mm. (A) For the oligomers with varying linker lengths: (red broken)  $\beta$ -Glc-3-10-TBS ( $1.5 \times 10^{-4}$  M), (blue solid)  $\beta$ -Glc-6-10-TBS ( $1.5 \times 10^{-4}$  M), and (black solid)  $\beta$ -Glc-12-10-TBS ( $1.5 \times 10^{-4}$  M). (B) For the oligomers with varying lengths of ethynylpyridine moiety and a different terminal group: (blue)  $\beta$ -Glc-3-14-TBS ( $1.1 \times 10^{-4}$  M), (red)  $\beta$ -Glc-3-10-TBS ( $1.5 \times 10^{-4}$  M), (green)  $\beta$ -Glc-3-6-TBS ( $2.5 \times 10^{-4}$  M), (black)  $\beta$ -Glc-3-3-TBS ( $5.0 \times 10^{-4}$  M), and (yellow)  $\beta$ -Glc-3-10-H ( $1.5 \times 10^{-4}$  M). The corresponding UV spectra are shown in Figure S2 in the Supporting Information.

**Table 2.** Molar Ellipticity for Glycoside-Linked Ethynylpyridine Oligomers Yyy-*m*-*n*-R' in  $\text{CH}_2\text{Cl}_2$ <sup>a</sup>

Yyy- <i>m</i>	$[\theta]_{\text{peak}} \times 10^{-4} / \text{mdeg dM}^{-1} \text{ cm}^{-1}$ ( $\lambda(\text{CD}_{\text{max}}) / \text{nm}$ )			
	Yyy- <i>m</i> -6-TBS	Yyy- <i>m</i> -10-TBS	Yyy- <i>m</i> -14-TBS	Yyy- <i>m</i> -10-H
$\beta$ -Glc-3	−1 (325)	−21 (336)	−23 (336)	−1 (325)
$\beta$ -Glc-6	−1 (331)	−24 (336)		
$\beta$ -Glc-12	−1 (325)	−22 (337)		
$\alpha$ -Glc-3	−5 (331)	−102 (337)	−65 (336)	−5 (333)
$\beta$ -Gal-3	−5 (331)	63 (337)	106 (337)	9 (336)
$\alpha$ -Gal-3	−3 (331)	85 (336)	82 (337)	6 (337)
$\alpha$ -Man-3	41 (337)	68 (338)	178 (338)	5 (340)

<sup>a</sup> Conditions: see the legends of Figures 4A and 5 and Figures S3–S6 in the Supporting Information. The CD and UV spectra for  $\alpha$ -glucosides,  $\alpha/\beta$ -galactosides, and  $\alpha$ -mannosides are shown in Figures S3–S7.

concentration of  $1.5 \times 10^{-3}$  M. Indeed, for the  $\alpha$ -mannoside-linked oligomers, the molar ellipticity and molar extinction coefficient of the band appearing at the longest wavelength changed considerably with increasing length of the ethynylpyridine moiety (Figure S6 in Supporting Information). In general, the longer oligomers have larger molar CD ellipticities  $[\theta]$  and smaller molar extinction coefficients after normalization by the number of pyridine units. This observation suggests that pyridine units of longer ethynylpyridine moieties will strongly interact with one another at an interval of one pitch of the resulting helices. It is noteworthy that  $\alpha$ -Man-3-14-TBS showed outstanding hypochromism resulting from the tightly wound helical structure, reminiscent of the formation of DNA duplexes from the corresponding single strands.<sup>1b</sup>



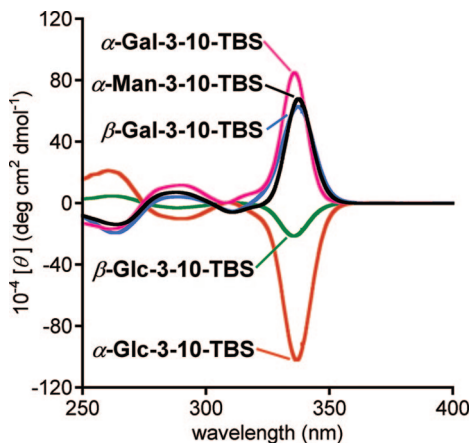


**Figure 5.** CD spectra of decamers linked with various glycosides. [Yyy-3-10-TBS] =  $1.5 \times 10^{-4}$  M in  $\text{CH}_2\text{Cl}_2$ , 25 °C, path length = 1 mm: (green)  $\beta$ -Glc-3-10-TBS, (orange)  $\alpha$ -Glc-3-10-TBS, (blue)  $\beta$ -Gal-3-10-TBS, (red)  $\alpha$ -Gal-3-10-TBS, (black)  $\alpha$ -Man-3-10-TBS.

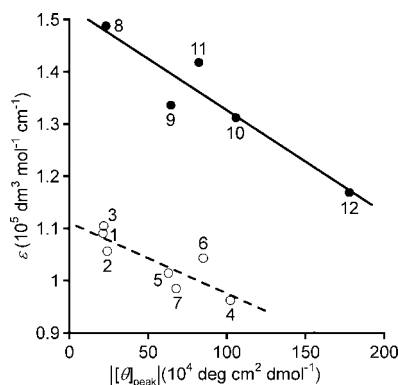


**Figure 6.** Relationship between molar extinction coefficient and absolute value of molar ellipticity at the peak of the longest wavelength. Open circle: decamers; filled circle: tetradecamers. 1:  $\beta$ -Glc-3-10-TBS, 2:  $\beta$ -Glc-6-10-TBS, 3:  $\beta$ -Glc-12-10-TBS, 4:  $\alpha$ -Glc-3-10-TBS, 5:  $\beta$ -Gal-3-10-TBS, 6:  $\alpha$ -Gal-3-10-TBS, 7:  $\alpha$ -Man-3-10-TBS, 8:  $\beta$ -Glc-3-14-TBS, 9:  $\alpha$ -Glc-3-14-TBS, 10:  $\beta$ -Gal-3-14-TBS, 11:  $\alpha$ -Gal-3-14-TBS, 12:  $\alpha$ -Man-3-14-TBS.

We thought that the molar extinction coefficients might correlate with the absolute values of the CD ellipticities within the oligomers possessing the same length of ethynylpyridine moiety regardless of the saccharides linked. When  $\epsilon$  was plotted against  $|\theta|$  for each group of glycoside-linked decamers (open circle in Figure 6) and tetradecamers (filled circles in Figure 6), rough negative correlations were observed for both groups. As  $\epsilon$  decreased,  $|\theta|$  increased, reflecting the effect with the type of glycoside: the more effective templates form the tighter helices and showed both stronger hypochromism and stronger Cotton effect more, as a result of shortening the interval between the turns of the helices.

**$^1\text{H}$  NMR Spectra of  $\alpha$ -Man-3-*n*-TBS.**  $^1\text{H}$  NMR spectra of the glycoside-linked oligomers were measured in  $\text{CDCl}_3$  and  $\text{CDCl}_3/\text{CD}_3\text{OD}$ . In  $\text{CDCl}_3$ , intramolecular association typically caused broadening of the NMR signals for aromatic and saccharide protons and downfield movement for saccharide C–H protons compared to those in  $\text{CDCl}_3/\text{CD}_3\text{OD}$ . For example, Figure 7 shows  $^1\text{H}$  NMR spectra of (A)  $\alpha$ -Man-3-10-TBS in  $\text{CDCl}_3$ , (B)  $\alpha$ -Man-3-10-TBS in  $\text{CDCl}_3/\text{CD}_3\text{OD}$  (2:1), and (C) HO-3-10-TBS in  $\text{CDCl}_3$ . The resemblance between panels B and C shows that the ethynylpyridine moiety in  $\alpha$ -Man-3-10-TBS becomes free from the mannoside template because hydrogen bonding is inhibited by the presence of  $\text{CD}_3\text{OD}$ . In Figure 7A, substantial changes were caused by

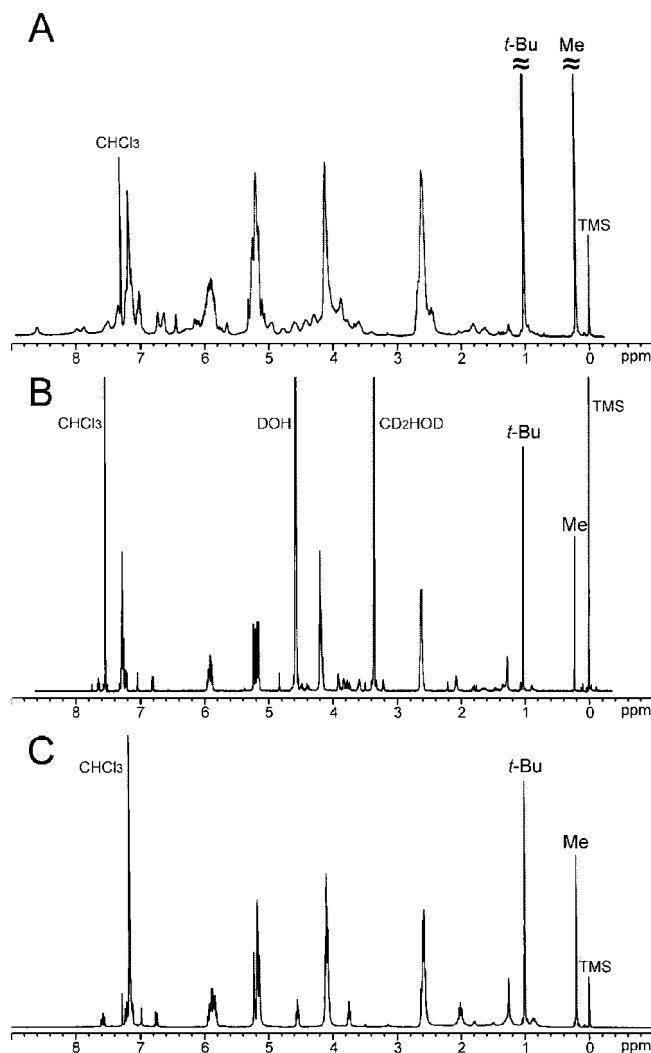


**Figure 7.**  $^1\text{H}$  NMR spectra for (A)  $\alpha$ -Man-3-10-TBS in  $\text{CDCl}_3$ , 300 MHz, (B)  $\alpha$ -Man-3-10-TBS in  $\text{CDCl}_3/\text{CD}_3\text{OD}$  (2:1), 500 MHz, and (C) HO-3-10-TBS in  $\text{CDCl}_3$ , 500 MHz. 23 °C. *t*-Bu and Me: sets of TBS signals; TMS = tetramethylsilane.

intramolecular hydrogen bondings: the signals become broadened, and some of them appeared at  $\delta$  = 8.6, 7.8–8.0, and 6.4–6.7 ppm. Although complete assignment of the signals is not attained, the emerging signals would be from the hydrogen-bonded O–H and/or C–H protons influenced by the anisotropic effect of the ethynylpyridine moiety.

The mannoside-linked oligomers displayed intense CD even for the short hexamer (Figure S6). When the NMR spectra for  $\alpha$ -Man-3-6-TBS were studied in detail, further interesting behavior was observed for its TBS terminal.  $^1\text{H}$  NMR spectra were measured in  $\text{CDCl}_3$ ,  $\text{CDCl}_3/\text{CD}_3\text{OD}$  (2:1) (Figure 8), and  $\text{CDCl}_3$  after treatment with  $\text{D}_2\text{O}$ , in order to specify exchangeable OH signals (Figure S8 in Supporting Information). For the  $^1\text{H}$  NMR spectra in  $\text{CDCl}_3$ , two sets of signals for *tert*-butyl and methyl groups in the TBS terminal were observed: one set indicates a usual TBS group (two singlets: 1.00 and 0.20 ppm), while the other showed a large upfield shift (0.71 and –0.38 ppm) with fine splitting of the methyl group into two signals (Figure 8A). Two sets of signals were also found for the joint pyridine ring attaching the linker (Figure 8A, filled and open triangles). On the other hand, in  $\text{CDCl}_3/\text{CD}_3\text{OD}$ , we observed only one pair of the TBS singlet signals (1.01 ppm for *t*-Bu, 0.22 ppm for Me) and one set of the pyridine signals (Figure 8B), resembling that of HO-3-10-TBS (Figure 7C). These findings indicate that in  $\text{CDCl}_3$  there are two stable structures

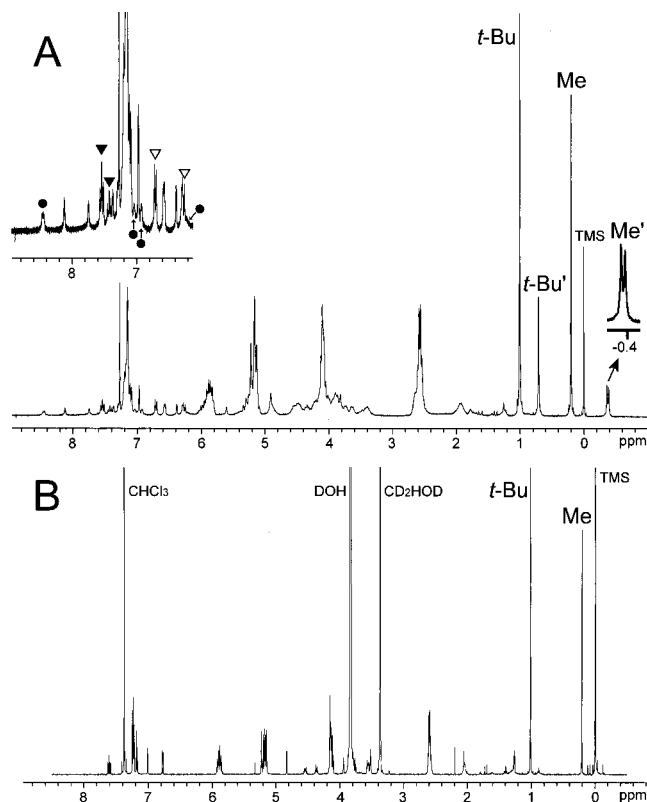


**Figure 8.**  $^1\text{H}$  NMR spectra for  $\alpha\text{-Man-3-6-TBS}$  (A) in  $\text{CDCl}_3$ , 23  $^\circ\text{C}$ , 300 MHz and (B)  $\text{CDCl}_3/\text{CD}_3\text{OD}$  (2:1), 23  $^\circ\text{C}$ , 500 MHz. In (A), filled circles indicate OH groups in an  $\alpha$ -mannoside template, and filled and open triangles indicate two sets of signals for 4-H and 3-H (*meta* and *ortho* to O) at the linker-attached pyridine ring; *t*-Bu and Me/*t*-Bu' and Me': sets of TBS signals; TMS = tetramethylsilane.

for the hydrogen-bonding intramolecular complexation in  $\alpha\text{-Man-3-6-TBS}$ . Indeed, the OH signals shifted downfield (Figure 8A, filled circle) as a result of the intramolecular hydrogen bonding. The two possible structures for the helical complexes are shown in Figure 9. The upper and lower figures display transoid and cisoid conformers, respectively, at the two terminal pyridine rings. In the transoid conformer, the TBS group is located outside the helix and receives no anisotropic effect. On the other hand, in the cisoid conformer, the TBS group overlaps the pyridine rings at an interval of one pitch of the helix and receives anisotropic effect that causes splitting of the two diastereotopic methyl groups in the TBS group, which is located at the opposite end to the saccharide moiety.

**Monte Carlo Molecular Mechanics Study.** The decamers  $\text{Yyy-3-10-TBS}$  ( $\text{Yyy} = \alpha\text{- and } \beta\text{-Glc, } \alpha\text{- and } \beta\text{-Gal, and } \alpha\text{-Man}$ ) were examined by Monte Carlo molecular mechanics optimization. Two types of initial structures based on P- and M-helices, in which the glycoside moiety was placed in the pore, were submitted for each decamer. The solvent was set as  $\text{CHCl}_3$ . During the optimization, helix inversion or collapsing was not observed; therefore, two types of energetically minimum structures corresponding to P- and M-helices were obtained for each decamer. In all optimized structures, the terminal TBS-acetylene group appeared in transoid conformation (Figure 9, top) even when the initial structure was submitted as a cisoid form. Hydrogen bonds stabilize helical structures, and their number was varied. The van der Waals interaction between pitches was observed for both the main pyridine-acetylene chains and side butenyloxy chains. Except for the M-helix of  $\alpha\text{-Man-3-10-TBS}$  and P-helix of  $\beta\text{-Glc-3-10-TBS}$ , one pitch of the helix consists of five pyridine rings and six acetylene bond, so that one pyridine ring overlaps with one acetylene bond

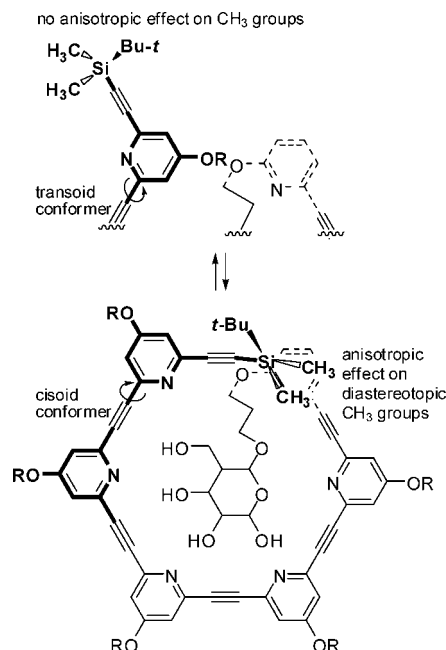


**Figure 9.** Possible structures of two conformers of  $\alpha\text{-Man-3-6-TBS}$ : (upper) transoid conformer and (lower) cisoid conformer.

over the pitch. The side chains interdigitate, and the TBS group takes part in the interdigitation to anchor the terminal of the oligomer. TBS groups might stabilize the helicity through this interaction. In the M-helix of  $\alpha\text{-Man-3-10-TBS}$  and P-helix of  $\beta\text{-Glc-3-10-TBS}$ , one pitch of the helix consists of five pyridine rings and five acetylene bonds, and one pyridine ring overlaps with another pyridine ring. Its side chains also make interacting pairs over the pitch. The optimized P- and M-helix forms of  $\alpha\text{-Man-3-10-TBS}$  are shown in Figure S9 in the Supporting Information. The differences in the calculated energy between  $E(\text{P-helix})$  and  $E(\text{M-helix})$  are large (10–14  $\text{kJ mol}^{-1}$ ) for the two glucosides and small ( $< 6 \text{ kJ mol}^{-1}$ ) for the mannoside and galactosides (Table S1 in the Supporting Information). It seems that the more stable M-helicity of glucosides corresponds to the (–)-CD signals shown in Figure 5.

## Conclusion

A new series of ethynylpyridine oligomers were developed, in which various glycoside templates were linked by a covalent bond to form stable helices. The primary structure of the oligomers, including the lengths of ethynylpyridine moieties and linkers and the types of terminal groups and saccharide templates, was varied. Intramolecular hydrogen bonding resulted in chiral helices, whose structures were found to depend strongly on the length of ethynylpyridines and the types of the terminal groups and the linked glycosides. The rigidity of the helices was roughly evaluated from the strength of induced CD and hypochromism in UV spectra. Furthermore, for the mannoside-linked hexameric oligomer, the two transoid and cisoid conformers were observed by NMR, and the terminal *tert*-butyldimethylsilyl group in the cisoid conformer remarkably received an anisotropic effect through one pitch of the resulting helix. The structural information on the chiral helices for their sense, pitch, and size was encoded on the primary structure of the oligomers.

**Supporting Information Available:** Whole experimental procedures, Figures S1–S9, Table S1, and  $^1\text{H}$  NMR spectra for new compounds. This material is available free of charge via the Internet at <http://pubs.acs.org>.

## References and Notes

- (1) (a) Schulz, G. E.; Schirmer, R. H. *Principles of Protein Structure*; Springer-Verlag: New York, 1979. (b) Saenger, W. *Principles of Nucleic Acid Structure*; Springer-Verlag: New York, 1984.
- (2) (a) Feiters, M. C.; Nolte, R. J. M. In *Advances in Supramolecular Chemistry*; Gokel, G. W., Ed.; JAI Press: Stamford, 2000; Vol 6, pp 41–156. (b) Yashima, E.; Okamoto, Y. In *Circular Dichroism—Principle and Applications*, 2nd ed.; Berova, N.; Nakanishi, K.; Woody, R. W., Eds.; Wiley-VCH: New York, 2000; pp 521–546. (c) *Foldamers*; Hecht, S.; Huc, I., Eds.; Wiley-VCH: Weinheim, 2007. (d) Cornelissen, J. J. L. M.; Rowan, A. E.; Nolte, R. J. M.; Sommerdijk, N. A. J. M. *Chem. Rev.* **2001**, *101*, 4039–4070. (e) Yashima, E.; Maeda, K.; Nishimura, T. *Chem.—Eur. J.* **2004**, *10*, 42–51. (f) Hembury, G. A.; Borovkov, V. V.; Inoue, Y. *Chem. Rev.* **2008**, *108*, 1–73.
- (3) (a) Hill, D. J.; Mio, M. J.; Prince, R. B.; Hughes, T. S.; Moore, J. S. *Chem. Rev.* **2001**, *101*, 3893–4011. (b) Nakano, T.; Okamoto, Y. *Chem. Rev.* **2001**, *101*, 4013–4038. (c) Schmuck, C. *Angew. Chem., Int. Ed.* **2003**, *42*, 2448–2452. (d) Huc, I. *Eur. J. Org. Chem.* **2004**, 17–29. (e) Ray, C. R.; Moore, J. S. *Adv. Polym. Sci.* **2005**, *177*, 91–149. (f) Maeda, K.; Yashima, E. *Top. Curr. Chem.* **2006**, *265*, 47–88. (g) Yashima, E.; Maeda, K. *Macromolecules* **2008**, *41*, 3–12. (h) Kim, H.-J.; Lim, Y.-B.; Lee, M. J. *Polym. Sci., Part A: Polym. Chem.* **2008**, *46*, 1925–1935.
- (4) (a) Ciardelli, F.; Lanzillo, S.; Pieroni, O. *Macromolecules* **1974**, *2*, 174–179. (b) Moore, J. S.; Gorman, C. B.; Grubbs, R. H. *J. Am. Chem. Soc.* **1991**, *113*, 1704–1712. (c) Yashima, E.; Huang, S.; Okamoto, Y. *J. Chem. Soc., Chem. Commun.* **1994**, 1811–1812. (d) Nomura, R.; Nakako, H.; Matsuda, T. *J. Mol. Catal. A: Chem.* **2002**, *190*, 197–205. (e) Prince, R. B.; Brunsveld, L.; Meijer, E. W.; Moore, J. S. *Angew. Chem., Int. Ed.* **2000**, *39*, 228–230. (f) Brunsveld, L.; Meijer, E. W.; Prince, R. B.; Moore, J. S. *J. Am. Chem. Soc.* **2001**, *123*, 7978–7984. (g) Zhao, X.; Schanze, K. S. *Langmuir* **2006**, *22*, 4856–4862. (h) Sugiura, H.; Nigorikawa, Y.; Saiki, Y.; Nakamura, K.; Yamaguchi, M. *J. Am. Chem. Soc.* **2004**, *126*, 14858–14864. (i) Sugiura, H.; Amemiya, R.; Yamaguchi, M. *Chem.—Asian J.* **2008**, *3*, 244–260. (j) Sinkeldam, R. W.; van Houtem, M. H. C. J.; Pieterse, K.; Vekemans, J. A. J. M.; Meijer, E. W. *Chem.—Eur. J.* **2006**, *12*, 6129–6137. (k) Tanatani, A.; Yokoyama, A.; Azumaya, I.; Takakura, Y.; Mitsui, C.; Shiro, M.; Uchiyama, M.; Muranaka, A.; Kobayashi, N.; Yokozawa, T. *J. Am. Chem. Soc.* **2005**, *127*, 8553–8561. (l) Sanji, T.; Sato, Y.; Kato, N.; Tanaka, M. *Macromolecules* **2007**, *40*, 4747–4749.
- (5) (a) Green, M. M. In ref 2b, pp 491–520. (b) Green, M. M.; Park, J.-W.; Sato, T.; Teramoto, A.; Lifson, S.; Selinger, R. L. B.; Selinger, J. V. *Angew. Chem., Int. Ed.* **1999**, *38*, 3138–3154.
- (6) (a) Stone, M. T.; Fox, J. M.; Moore, J. S. *Org. Lett.* **2004**, *6*, 3317–3320. (b) Kolomiets, E.; Berl, V.; Lehn, J.-M. *Chem.—Eur. J.* **2007**, *13*, 5466–5479. (c) Dolain, C.; Maurizot, V.; Huc, I. *Angew. Chem., Int. Ed.* **2003**, *42*, 2738–2740. (d) Maurizot, V.; Dolain, C.; Huc, I. *Eur. J. Org. Chem.* **2005**, 1293–1301. (e) Dolain, C.; Jiang, H.; Léger, J.-M.; Guionneau, P.; Huc, I. *J. Am. Chem. Soc.* **2005**, *127*, 12943–12951. (f) Buffeteau, T.; Ducasse, L.; Poniman, L.; Delsuc, N.; Huc, I. *Chem. Commun.* **2006**, 2714–2716. (g) Jha, S. K.; Cheon, K.-S.; Green, M. M.; Selinger, J. V. *J. Am. Chem. Soc.* **1999**, *121*, 1665–1673. (h) Tabei, J.; Shiotsuki, M.; Sato, T.; Sanda, F.; Masuda, T. *Chem.—Eur. J.* **2005**, *11*, 3591–3598. (i) Nath, G. Y.; Samal, S.; Park, S.-Y.; Murthy, C. N.; Lee, J.-S. *Macromolecules* **2006**, *39*, 5965–5966. (j) Pijper, D.; Feringa, B. L. *Angew. Chem., Int. Ed.* **2007**, *46*, 3693–3696.
- (7) Becerril, J.; Rodriguez, J. M.; Saraogi, I.; Hamilton, A. D. In ref 2c, pp 195–228.
- (8) (a) Green, M. M.; Reidy, M. P.; Johnson, R. D.; Darling, G.; O’Leary, D. J.; Willson, G. *J. Am. Chem. Soc.* **1989**, *111*, 6452–6454. (b) Nagai, K.; Maeda, K.; Takeyama, Y.; Sato, T.; Yashima, E. *Chem.—Asian J.* **2007**, *2*, 1314–1321. (c) Kobayashi, S.; Morino, K.; Yashima, E. *Chem. Commun.* **2007**, 2351–2353. (d) Maeda, K.; Tsukui, H.; Matsushita, Y.; Yashima, E. *Macromolecules* **2007**, *40*, 7721–7726. (e) Miyagawa, T.; Yamamoto, M.; Muraki, R.; Onouchi, H.; Yashima, E. *J. Am. Chem. Soc.* **2007**, *129*, 3676–3682. (f) Goto, H.; Furusho, Y.; Yashima, E. *J. Am. Chem. Soc.* **2007**, *129*, 9168–9174. (g) Kakuchi, R.; Sakai, R.; Otsuka, I.; Satoh, T.; Kaga, H.; Kakuchi, T. *Macromolecules* **2005**, *38*, 9441–9447. (h) Prince, R. B.; Barnes, S. A.; Moore, J. S. *J. Am. Chem. Soc.* **2000**, *122*, 2758–2762. (i) Tanatani, A.; Mio, M. J.; Moore, J. S. *J. Am. Chem. Soc.* **2001**, *123*, 1792–1793. (j) Nishinaga, T.; Tanatani, A.; Oh, K.; Moore, J. S. *J. Am. Chem. Soc.* **2002**, *124*, 5934–5935. (k) Stone, M. T.; Moore, J. S. *Org. Lett.* **2004**, *6*, 469–472. (l) Goto, K.; Moore, J. S. *Org. Lett.* **2005**, *7*, 1683–1686. (m) Hou, J.-L.; Shao, X.-B.; Chen, G.-J.; Zhou, Y.-X.; Jiang, X.-K.; Li, Z.-T. *J. Am. Chem. Soc.* **2004**, *126*, 12386–12394. (n) Yi, H.-P.; Shao, X.-B.; Hou, J.-L.; Li, C.; Jiang, X.-K.; Li, Z.-T. *New J. Chem.* **2005**, *29*, 1213–1218. (o) Li, C.; Ren, S.-F.; Hou, J.-L.; Yi, H.-P.; Zhu, S.-Z.; Jiang, X.-K.; Li, Z.-T. *Angew. Chem., Int. Ed.* **2005**, *44*, 5725–5729. (p) Hou, J.-L.; Yi, H.-P.; Shao, X.-B.; Li, C.; Wu, Z.-Q.; Jiang, X.-K.; Wu, L.-Z.; Tung, C.-H.; Li, Z.-T. *Angew. Chem., Int. Ed.* **2006**, *45*, 796–800.
- (9) (a) Inouye, M.; Waki, M.; Abe, H. *J. Am. Chem. Soc.* **2004**, *126*, 2022–2027. (b) Abe, H.; Masuda, N.; Waki, M.; Inouye, M. *J. Am. Chem. Soc.* **2005**, *127*, 16189–16196. (c) Waki, M.; Abe, H.; Inouye, M. *Chem.—Eur. J.* **2006**, *12*, 7639–7647. (d) Waki, M.; Abe, H.; Inouye, M. *Angew. Chem., Int. Ed.* **2007**, *46*, 3059–3061.
- (10) For saccharide recognition by synthetic hosts, see: (a) Penadés, S., Ed.; *Host-Guest Chemistry—Mimetic Approaches to Study Carbohydrate Recognition*. *Top. Curr. Chem.* Vol. 218; Springer-Verlag: Berlin; 2002. (b) Davis, A. P.; Wareham, R. S. *Angew. Chem., Int. Ed.* **1999**, *38*, 2978–2996. See also refs 8f, 8m, and 8n.
- (11) Klapars, A.; Buchwald, S. L. *J. Am. Chem. Soc.* **2002**, *124*, 14844–14845.
- (12) Curran, D. P.; Liu, H.; Josien, H.; Ko, S.-B. *Tetrahedron* **1996**, *52*, 11385–11404.
- (13) (a) Nelson, J. C.; Saven, J. G.; Moore, J. S. *Science* **1997**, *277*, 1793–1796. (b) Prince, R. B.; Saven, J. G.; Wolynes, P. G.; Moore, J. S. *J. Am. Chem. Soc.* **1999**, *121*, 3114–3121. (c) Lahiri, S.; Thompson, J. L.; Moore, J. S. *J. Am. Chem. Soc.* **2000**, *122*, 11315–11319. (d) Ohkita, M.; Lehn, J.-M.; Baum, G.; Fenske, D. *Chem.—Eur. J.* **1999**, *5*, 3471–3481. (e) Hecht, S.; Khan, A. *Angew. Chem., Int. Ed.* **2003**, *42*, 6021–6024.

MA801470R